J.J. OAK*[#], Y.C. LEE**, Y.H. PARK***

STRUCTURAL PROPERTIES AND MECHANICAL BEHAVIOR OF THE 2 STEP-REINFORCED Al-Si/SiC$_p$ METAL MATRIX COMPOSITE BY TITANIUM-FIBER

In this study, the newly designed Al-9Si/SiC particles (SiC$_p$) + Ti-fiber (2step-reinforced Al-9Si alloy matrix) metal matrix composites (MMCs) were fabricated by hot-pressing sintering at 560°C. 2step-reinforced Al-based MMCs were characterized by thermal shrinkage, phase transition, microstructure and tensile strength. The addition of Ti-fiber reduced thermal shrinkage was caused by temperature difference in sintering process as well as enhanced assistance for tensile strength and plastic deformation at room temperature. Experimental results reveal that the 2step-reinforcment sintering by ceramic and metal has a significant effect to increase interface bonding in boundary of each component material and the improved mechanical properties were due to the influence of interfacial product by diffusion. Tensile strength and elongation at room temperature by 2step-reinforcement were improved in 19.5% and 26.2% more than those of Al-9Si/ SiC$_p$, respectively. Especially, it reveals that diffusion direction may be varied by sintering methods at low temperature in this study.

Keywords: Metal matrix composite, Sintering, Ti fiber, Mechanical property, Diffusion

1. Introduction

Aluminum (Al) and its alloys due to low density, high-specific strength, remarkable malleability, excellent castability and high corrosion resistance have been rapidly required and developed for the continued growth in automotive industry [1-3]. In addition, these materials in use are produced by inexpensive manufacturing process is essential for mass production as like casting and powder metallurgy (PM) process [4-7]. Especially, improving vehicle weight and thereby fuel efficiency aspect at the same time of these materials, Al-Si based alloys is well-known as a casting alloy have been widely used in the transportation industry due to advantage with low cost, high corrosion resistance, wear resistance, liquidness fluidity in casting and shrinkage. Al-Si alloys with Si for hypoeutectic and eutectic composition have been improved to increase mechanical properties by which are precipitation of Al-Si eutectic-like phase and crystallization of primary Si phase [8]. Unfortunately, mechanical properties and weldability aspects of these materials for automotive partials, it is not as good [9].

Recently, it has been attempted to enhance mechanical properties in Al-Si matrix by isotropic properties and interfacial product [10]. These methods are the widely used in the improved structural strength from ceramic reinforcements such as SiC, Al$_2$O$_3$ and graphite [11-14]. Especially, these alloys and commercial Al-based alloy by powder metallurgy have a near-net shaping property in manufacturing process for parts of automotive application [15-17]. Unfortunately, it however still needs further improvement of low wettability between matrix material and ceramic reinforcement and surface modification of oxide layer on matrix material in manufacture of metal matrix composite (MMC) [18,19]. Li et al. observed solid state diffusion between Al-Si alloy and Ti at low temperature [20]. It has been dealt with the interfacial reacted Ti$_7$Al$_5$Si$_{12}$ phase and the related Ti(Al,Si) phases by diffusion couple. And Dezellus et al. reported formation of these phases by liquid-solid phase equilibria in Al-Si-Ti ternary system [21]. These scientific reports phase transformation on the Al-rich corner-based of the Al-Si-Ti ternary system. In the solubility of Ti, it was reported low amount of Ti into Al-Si matrix in casting process [22]. In case of Al-based power metallurgy, it however was no reports phase formation with diffusion behavior on Ti-rich and Al-rich corner-based of the Al-Si-Ti ternary system at same time.

The aim of this study is improvement of strength and plastic deformation of Al-based MMC by modified interface bonding between Al-Si matrix powders with SiC$_p$ as the primary-reinforcement and Ti-fiber as the second-reinforcement [23,24] as well as observation and control of relationship of phase formation behavior between Ti-rich and Al-rich corner-based effect and various sintering methods at low temperature region. Ti-fiber is

*   MATERIAL ANALYSIS LABORATORY, DAE-IL CORPORATION, 8, BONGGYENONGGONG-GIL, DUDONG-MYEON, ULJU-GUN, ULSAN 44914, REPUBLIC OF KOREA
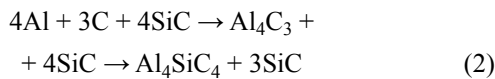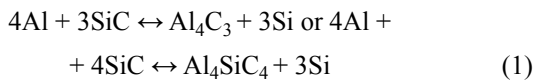**   KOREA INSTITUTE OF INDUSTRIAL TECHNOLOGY, BUSAN, REPUBLIC OF KOREA
*** DEPARTMENT OF MATERIALS SCIENCE AND ENGINEERING, PUSAN NATIONAL UNIVERSITY, BUSAN, REPUBLIC OF KOREA

[#]   Corresponding author: ojj69@dicorp.co.kr

expected to work efficiently for improving interface bonding in Al-Si/SiC$_p$ matrix by diffusion based on native values for mutual mixing enthalpy between Al-Ti and Si-Ti binary systems, and low thermal expansion of Ti-fiber is capable of controlling shrinkage of sintered body during the cooling process. In this study, the modified interface boundary of the sintered Al-based MMC by Ti-fiber reinforcement is reviewed. Furthermore, the upgraded mechanical properties in the sintered Al-Si/SiCp+Ti fiber MMCs and diffusion mechanism by various sintering methods were discussed in detail.

2. Experimental methods

Fig. 1 explains schematic illustration of design concept in Al-based MMC with Ti-fiber in this study. Initial powder materials were designed by the 1-step reinforced microstructure of the atomized Al-based MMCs in Fig. 1b as in-situ type blending and the 2-step reinforced microstructure of Al-based MMC with Ti-fiber in Fig. 1c as interfacial reacted type blending. Prior to preparation of Al-Si/SiCp powders with Ti-fibers (TF340, KOGI, Japan), 20 vol. % SiC particles with size of 10-20 μm were added in molten Al-9wt. % Si alloy at below 1000°C due to fusional reaction between Al-Si matrix and SiCp as follows[25,26].

$$4Al + 3SiC \leftrightarrow Al_4C_3 + 3Si \text{ or } 4Al + \\ + 4SiC \leftrightarrow Al_4SiC_4 + 3Si \quad (1)$$

$$4Al + 3C + 4SiC \rightarrow Al_4C_3 + \\ + 4SiC \rightarrow Al_4SiC_4 + 3SiC \quad (2)$$

It is well-known as brittle phases, Al$_4$C$_3$ and Al$_4$SiC$_4$, are to reduce the interfacial bonding strength. Especially, the poor corrosion resistance in humid environment of occurs to limitations on the use of as a partial unit in vehicle application as follows.

$$Al_4C_3 + 12 H_2O \rightarrow 4Al (OH)_3 + 3CH_4 \quad (3)$$
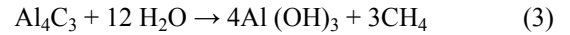
These reactions have to be considered to prevent above by-products in fabrication of SiC$_p$ reinforced composites based on Al-based alloys. The mixed materials in-situ state were atomized by inner gas with dynamic pressure of 2 MPa under 80% N$_2$ and 20% O$_2$ gas condition [27,28]. And then, the atomized Al-Si/SiCp powders and Ti fibers with 1 mm×20 μm were blended by turbulent mixer with 45rpm speed for 24hours. The proposed mixing ratio is from 0 to 25 wt. % Ti fiber in whole matrix. For establishment of sintering condition, thermal behavior of the mixed material was observed by differential thermal analysis (DTA: TG/DTA 7300, Seiko, Japan) with a heating rate of 10°C/min in an inert Ar gas flow atmosphere. Prior to sintering process of Al-Si/SiCp powders with Ti-fibers, sintering of pre-compaction of the mixed powders was carried out for estimation of effect in shrinkage and consolidation by sintering atmosphere. And then, the mixed powders were consolidated by hot press technique with isothermal heat treatments in vacuum atmosphere for 3×10^{-6} torr, during heating rate of 10°C/min with pressure for 70MPa. This process was consisted with at 200°C for 10 mins, 400ºC for 10 mins and 560°C for 1hr as shown in Fig. 2. The proposed isothermal heat treatment condition is based upon the DTA trace which has endothermic events and exothermic events with phase transformations between 530°C and 600°C as shown in Fig. 3. Sintering process was carried out by solid diffusion between Al-based MMC with an initial flow-viscosity region (heating zone I) and Ti-fiber as reinforcement. Cooling process for sintered specimens was adopted furnace cooling because this zone is on-set point of flow-viscosity and phase transformation zone from cooling zone I to cooling zone II in DTA trace. Phases
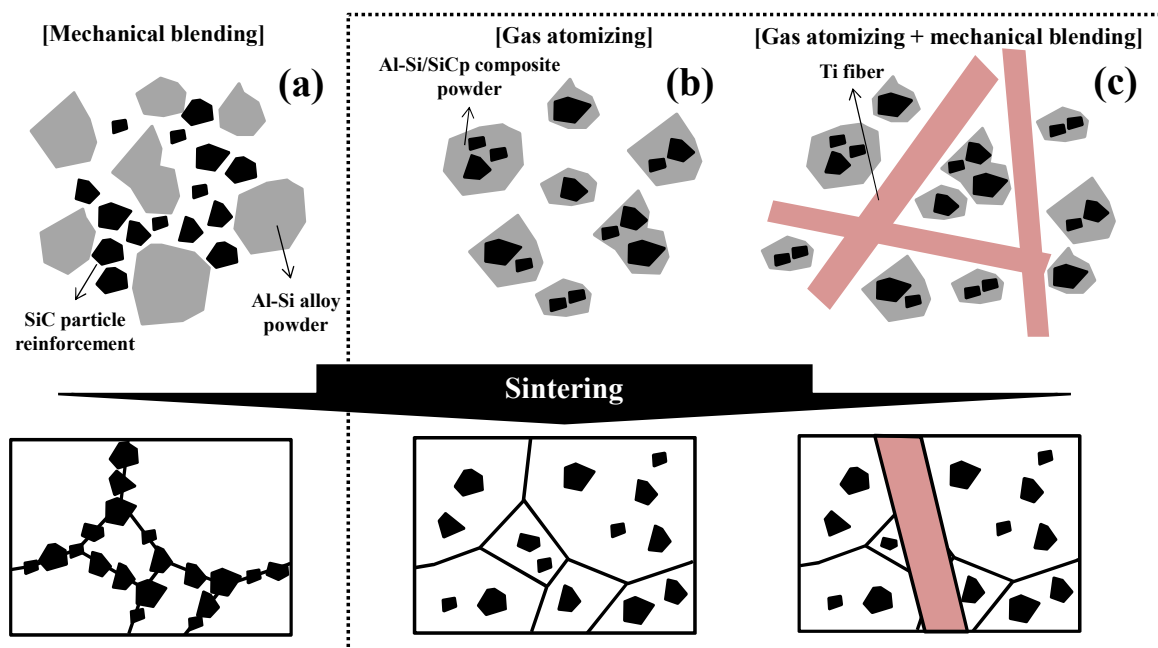

Fig. 1. Schematic illustration of the 1-step reinforced microstructure of the mechanical blended Al-based MMCs (a), the 1-step reinforced microstructure of the atomized Al-based MMCs (b) and the 2-step reinforced microstructure of Al-based MMC with Ti-fiber (c)
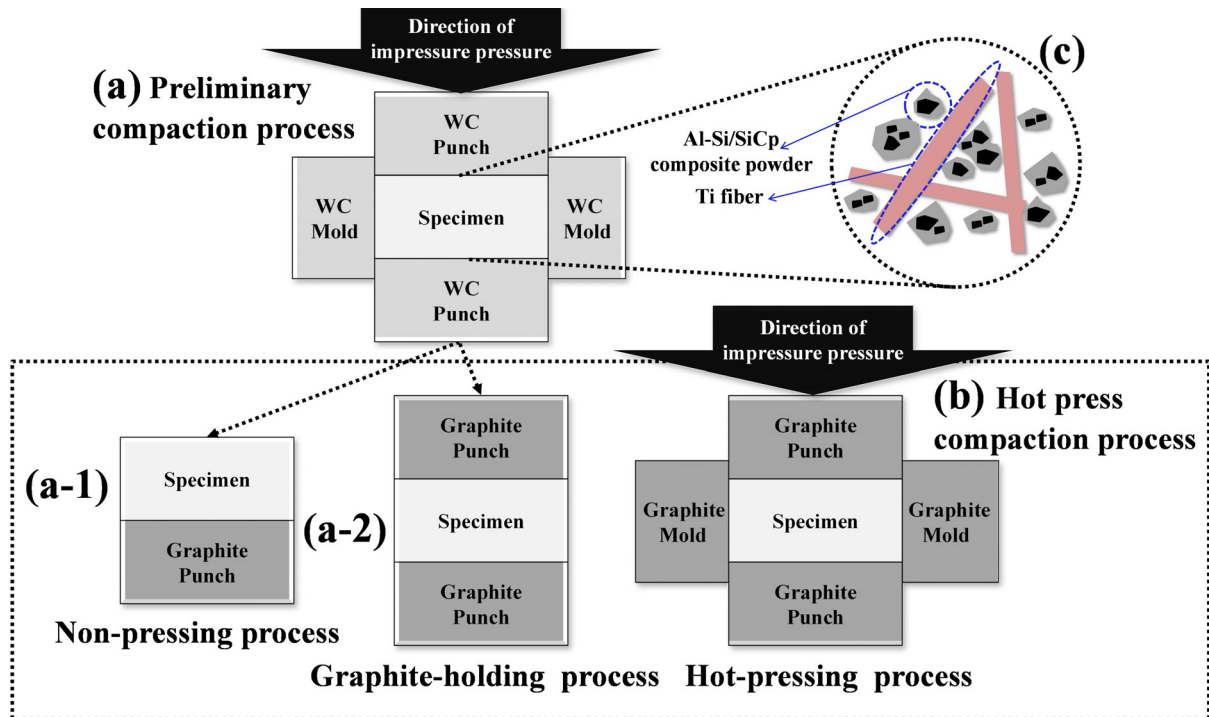
Fig. 2. Schematic illustration of the preliminary compaction sintering process (a, a-1, a-2), the hot press compaction sintering process (b) and the initial microstructure of Ti-fiber/metal matrix composites (c) before sintering process
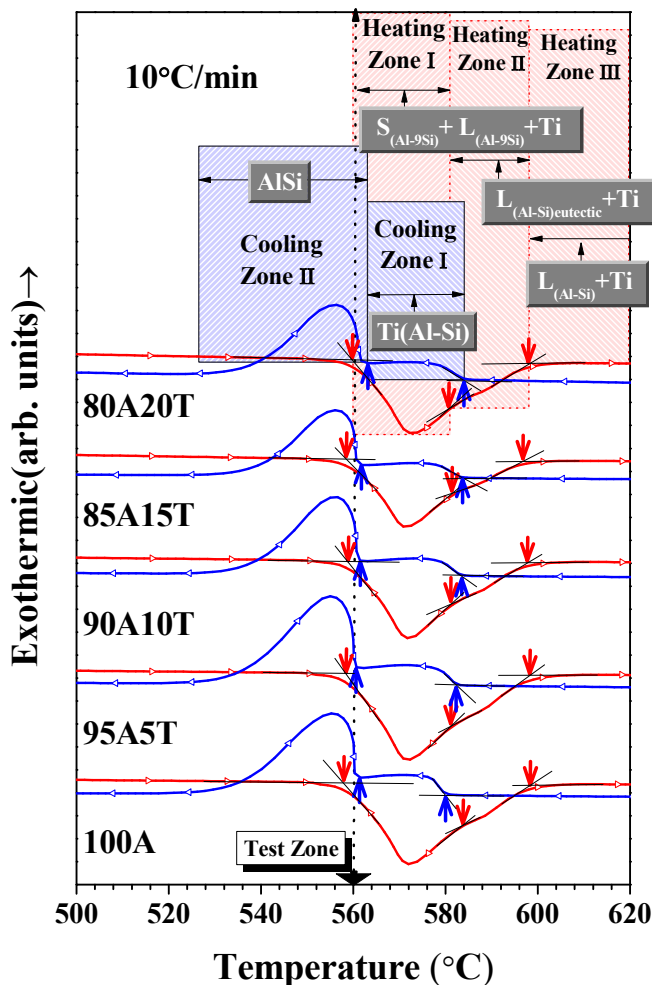

Fig. 3. DTA trace of the initial powders and the mixed powders with a heating rate of 10°C /mim.

characterization of each powder and sintered specimens were identified by X-Ray Diffraction (XRD: Ultima IV, Japan) using CuKα radiation at 30 kv, 40 mA for a 2θ range of from 20 to 80 degree. Microstructure of these materials were evaluated by optical microscopy (OM) and field emission-scanning electron microscope (FE-SEM: MIRA II LMH; Tescan, Brno, Czech Republic) with energy dispersive X-ray spectroscopy (EDS) analysis system. Mechanical properties of the sintered speci-mens were evaluated by Instron type universal tensile machine with strain rate for $5 \times 10^{-4} s^{-1}$ at room temperature. The tensile specimens were prepared to standard dimensions with ASTM E8-subsize. Prior to tensile test, all specimens were polished mechanically with SiC paper up to grit #2400 and then mounted strain gauge onto the test specimens in the gauge dimensions with 2.0×2.0×13.2 mm. Fracture surface of the tested specimens were observed by SEM.

3. Results and discussion

Fig. 4 shows the microstructures of the Al-based MMC powder with SiCp and Ti-fiber. The atomized Al-based MMC powder has an elliptical shape that is typical morphology by rapid atomization. SiCp in Al-based alloy matrix are evenly dispersed without clustering of SiCp. Al and Si are homogeneously ob-served without trace of segregation in Fig. 4b,c. Especially, Ai-Si eutectic-like network structural phase and primary Al phase are well developed in rapid quenched powder as shown in Fig. 4e. The used Ti-fiber has a single phase in Fig. 4f.

Fig. 5 shows each sinterability by sintering method and amount of Ti-fiber. In case of sintering method, the graphite-
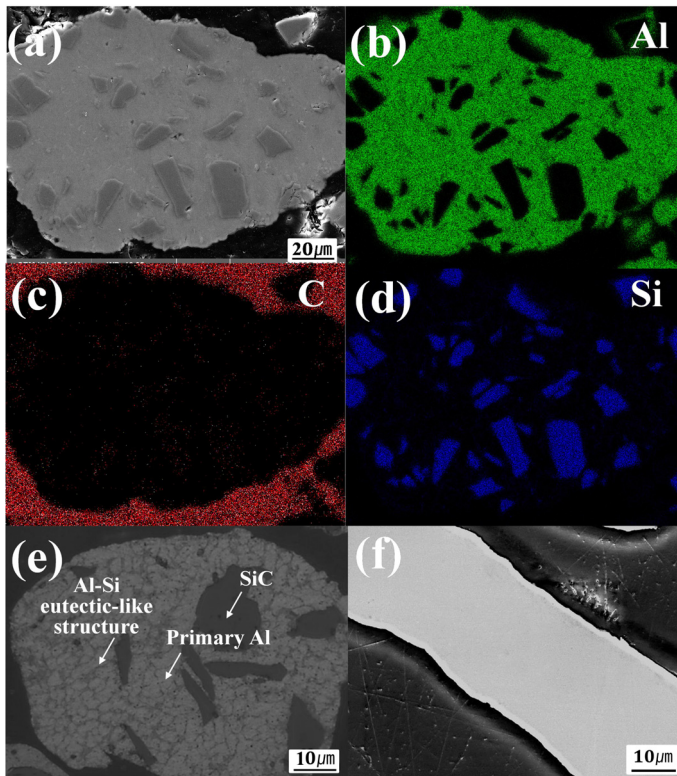
Fig. 4. Cross-section images of atomized AlSi/SiC powder (FE-SEM image: (a), mapping analysis for (a): (b), (c) and (d), OM image: (e)) and Ti-fiber (FE-SEM image: (f)).

holding process in Fig. 1(a-2) and the hot pressing process in Fig. 1b clearly show that existing effectively control shrinkage than the non-pressing process in Fig. 1(a-1). In case of effect in amount of Ti-fiber, the related shrinkage improved by increas-

ing amount of Ti-fiber in each sintering method in Fig. 5b. This phenomenon is observed by lateral morphologies in Fig. 5a, as shown in length difference between topside and bottom side is possible to evaluate with naked eye. Especially, it has a marked effect to control of shrinkage in 15 wt. % Ti-fiber content, regardless of sintering method.

The phases in the sintered specimens by each sintered method form initial materials are characterized by identification evaluation based on XRD patterns in Fig. 6. Initial materials are consisted of single α-phase Ti from Ti-fiber and α-Al, Si and SiC from Al-Si/SiCp in Fig. 6a. It means that atomized Al-Si/SiCp powders were fabricated as planned because the formation of undesirable Al_4C_3 or Al_4SiC_4 phase were not detected in this study. In case of phase transition in all sintered specimens, there are two difference phase formation behaviors which were classified by the formation of $Ti_7Al_5Si_{12}$ ternary phase or not during the sintering process. In the non-pressed and the graphite-holded sintering process, formation of these ternary phases with addition of Ti-fiber was observed as shown in Fig. 6b,c. On the other hand, it is revealed that hot-pressed specimens have simple-combined phase of Ti-fiber and phases of Al-Si/SiCp in Fig. 6d. It seems to be that forcibly accelerated flow-viscosity by the used compressive pressure with 70MPa induced product-inhibited sintering process to $Ti_7Al_5Si_{12}$ ternary phase despite input of 20 wt. % Ti-fibers.

Fig. 7 shows microstructure of the sintered specimens. Significant pores in the non-pressed specimens in (Fig. 7a) between matrix and Ti-fiber was observed. Main matrix materials clustered together in and around of SiCp and Ti-fiber. Amount of pores and clustering of matrix materials in and around Ti-fiber increased with Ti-fiber content increase. But to the
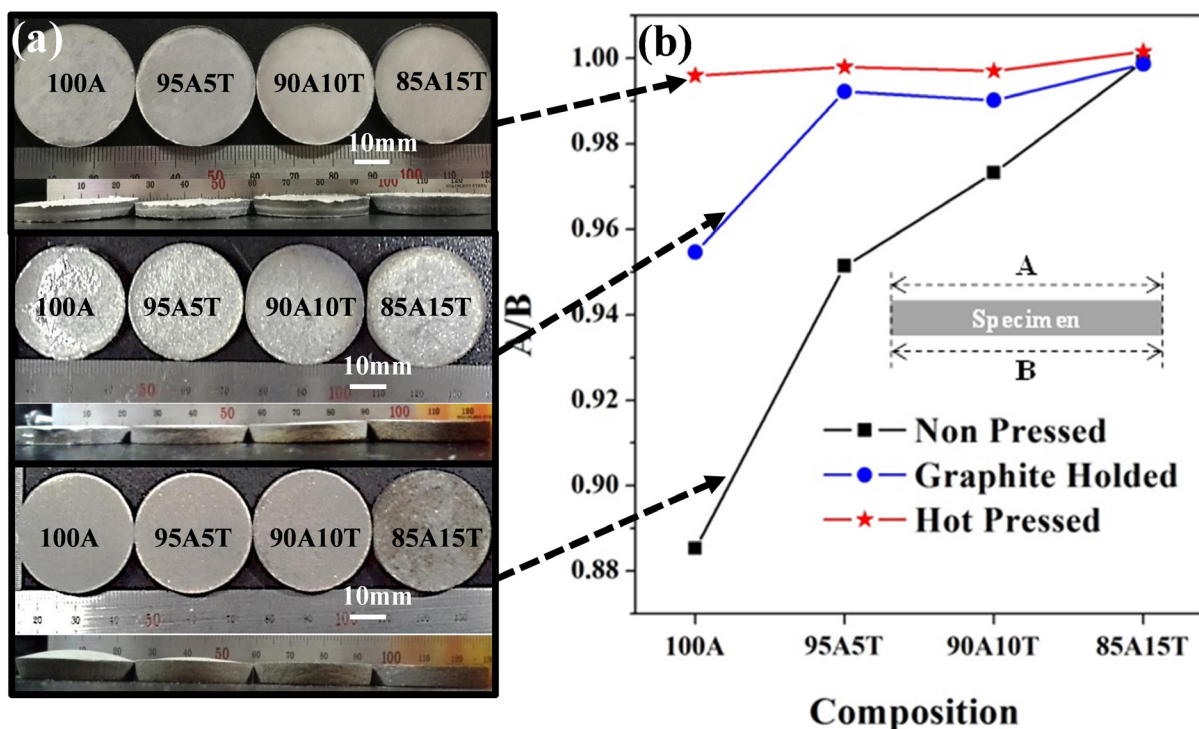

Fig. 5. Out-morphologies (a) and related shrinkages (b) of the sintered specimens by sintered method and effect of Ti-fiber
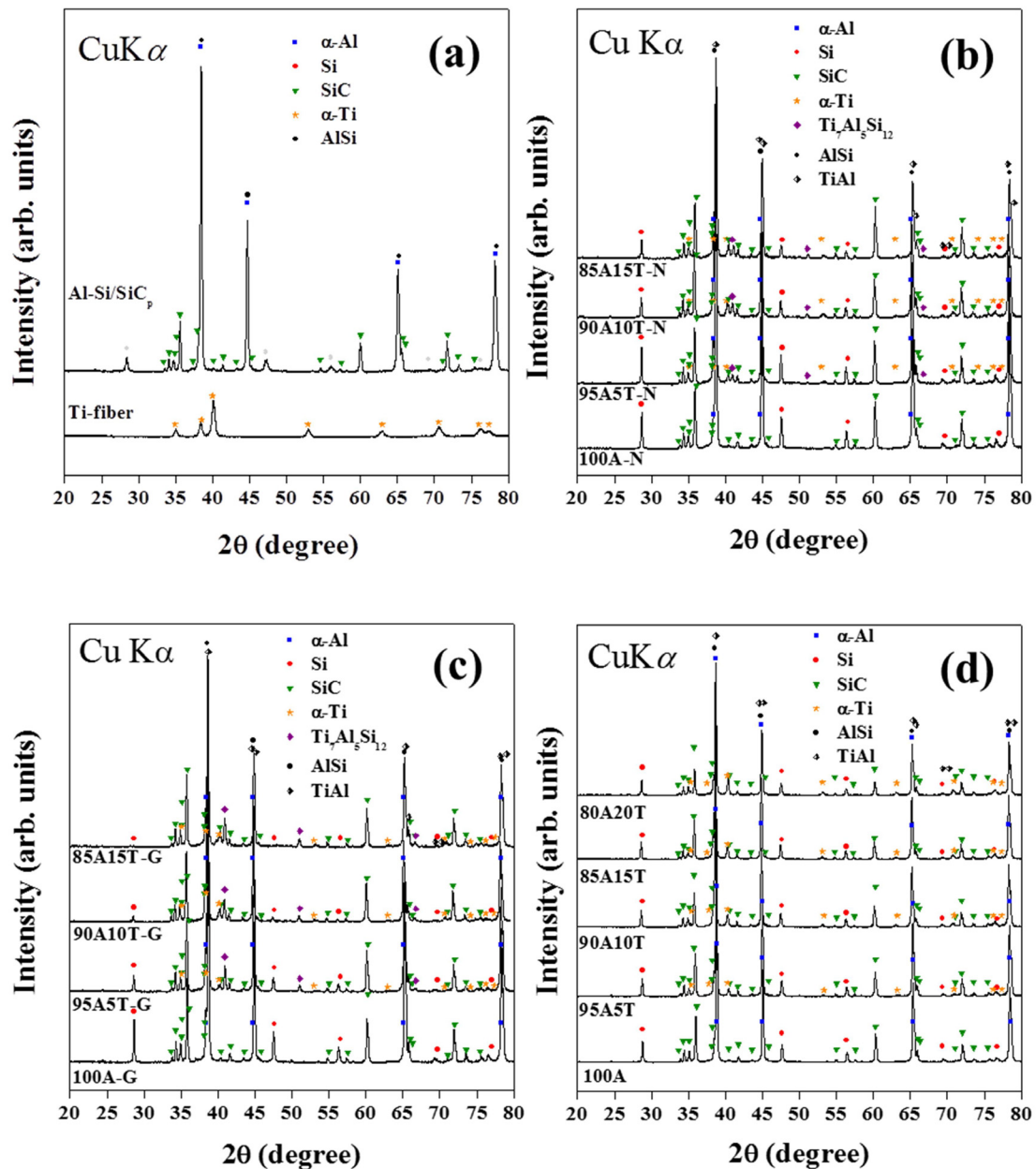
Fig. 6. XRD patterns of initial materials (a) and sintered specimens by each sintering method: (b) non-pressed specimens, (c) graphite-holed specimens and (d) hot-pressed specimens

contrary, matrix materials decreased in and around SiCp. The phenomenon causes deterioration in strength of Al-based MMCs because the used matrix materials have to be able to withstand the load-bearing in elastic deformation and to spread the load on the reinforcement at the same time. The interfacial reaction observed on layers contrasted between main matrix and Ti-fiber. These layers have ternary phase, Ti-Al-Si, was estimated by EDS line scanning. 85A15N specimen shows another reacted layer between Ti-fiber and ternary phase layer. This layer has an Al-rich phase than those of 95A5T and 90A10T. In case of the graphite-holed specimens in Fig. 7b, tendency of sinter-ability, clustering of matrix materials in and around Ti-fiber and the interfacial reacted layers shows similar with those of the non-pressed specimens. The maximum sintered density in the non-pressed and graphite-holed specimens was shown at each

95A5T specimen. These sinterabilities are similar with those of each 100A in Fig. 7a,b. In case of the hot-pressed specimens show highly-densed overall in Fig. 7c, the interfacial reacted layers have distinctly different formation behavior there is an obvious contrast between the hot-pressed specimen layers and those of the non-pressed and graphite-holed specimens. There are no significant formations with ternary phase layer such as each the interfacial reacted region as shown in Fig. 7a,b. Con-tinuously pressed main matrix with high flow-viscosity in and around solid Ti-fiber does not involve intermetallic phase at whole interfacial zone. The increased local thermal stress and flow-viscosity generated different diffusion behavior between Ti-fiber and main matrix, and accelerated dispersibility of SiCp lead to heterogeneous phase growth as shown in the SEM-EDS line scanning results of Fig. 7c. Results of qualitative analysis in
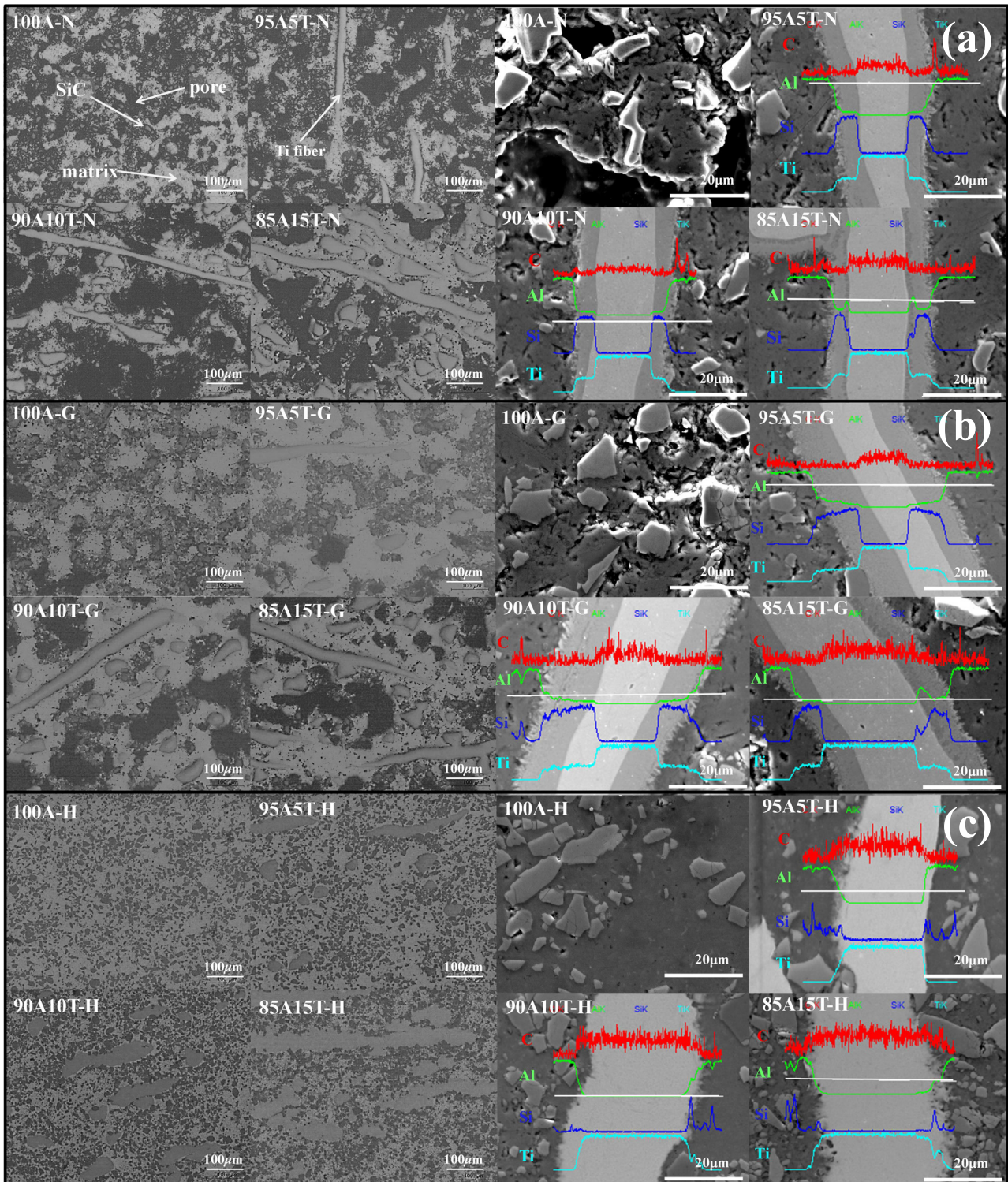
Fig. 7. FE-SEM micrographies and qualitative analysis of the sintered specimens by each sintering method: (a) non-pressed specimens, (b) graphite-holed specimens and (c) hot-pressed specimens

all the interfacial layers indicate that the produced intermetallic composites are good agree with the detected phases of XRD in Fig. 6.

Table 1 arranges record of mechanical properties of all specimens by each sintering method. It could be ascertained effect of Ti-fiber in non-pressed and graphite-holed sintering method and each 5 wt.% Ti-fiber added specimen in this study shows comparable mechanical properties with those of other specimens. Especially, improved elongation in elastic deformation region is observed for the sintered specimens containing 5 wt.% Ti-fiber. Unfortunately, plastic deformation of these sintered specimens was not observed. It seems deficiency of compaction in sintered specimens might be the cause in Fig. 7a,b. In care of the hot-pressed specimens, it could be ascertained the improved mechanical properties, strength and ductilization, originated with increase of amount of Ti-fiber.

TABLE 1

Mechanical property of the sintered specimens in this study

	Composition	UTS (MPa)	Y.S (MPa)	Elongation (%)	Elastic Modulus (GPa)
Non-pressed	100A	26	—	0.10	31.5
	95A5T	51	—	0.40	41.9
	90A10T	39	—	0.33	27.1
	85A15T	30	—	0.22	29.4
Graphite-holed	100A	101	—	0.17	65.1
	95A5T	98	—	0.36	48.5
	90A10T	45	—	0.21	22.3
	85A15T	41	—	0.26	18.4
Hot-pressed	100A	195	135.7	6.22	83.8
	95A5T	218	142.7	7.40	71.1
	90A10T	218	152.8	7.85	82.1
	85A15T	233	157.2	7.78	128.2
	80A20T	234	158.8	5.41	143.5

Fig. 8 explains fracture behavior by lateral morphologies of tensile tested specimens have the highest strength in each sintering method. Fracture behaviors of all specimens are characterized by interfacial failure and transgranular fracture. The non-pressed and graphite-holed containing each 5 wt.% Ti-fibers shows interfacial failure and transgranular fracture at the same time, respectively. Especially, the graphite-holed specimen has wider interfacial reaction layer than that of the non-pressed specimen as shown in Fig. 7a, and it was observed that volume of Ti-fiber matrix was decreased in a corresponding degree of volume of Ti-fiber matrix in the non-pressed specimen. The reacted layer has strongly contributed tensile strength even though the non-pressed

specimen has significant pores as shown in Fig. 7b and Fig. 8a. In addition, this ternary intermetallic layer reveals that has enough strength to lead transgranular fracture of Ti-fiber. In case of the hop-pressed specimen with 15 wt.% Ti-fibers, it observed interfacial failure behavior, highly densified SiCp clustering around Ti-fiber and fully compacted matrix. As results, there are two partial reinforcement effects. One is the intergrated interfacial reaction product by diffusion mechanism occurred from Al-Si matrix with flow-viscosity into solid Ti-fiber matrix as shown in schematic illustration ① of Fig. 8b. Another is the increased mobility of SiCp into Ti-fiber by the increased flow-viscosity of Al-Si matrix during hot-press process as shown in schematic illustration ② of Fig. 8c. Especially, the latter mechanism shows outstanding effectiveness to improve tensile strength and plastic deformation in this study.

This phenomenon well explains in Fig. 9 and Table 2. It is not enough amount of SiCp around Ti-fiber and strength of main matrix in graphite-holed specimen (Fig. 9a)) than those of hot-pressed specimen in Fig. 9b. For $Ti_7Al_5Si_{12}$ phase as the integrated interfacial reaction product to be supported structure for the load-bearing matrix, it needs sequential layer structure with balance strength for stress dispersion. By contrast, hot-pressed specimen satisfied the requirements due to the synthesized TiAl and AlSi phase supplied the applied stress with mobile distributed environment towards the reinforcements. Therefore, these results became the cause leading to the improved plastic deformation in the hot-pressed specimens. In formation of the interfacial reaction produce, experimental results indicate two difference phase formation behaviors were classified by $Ti_7Al_5Si_{12}$ ternary phase in Fig. 6(b-c) or not Fig. 6d during the sintering process.
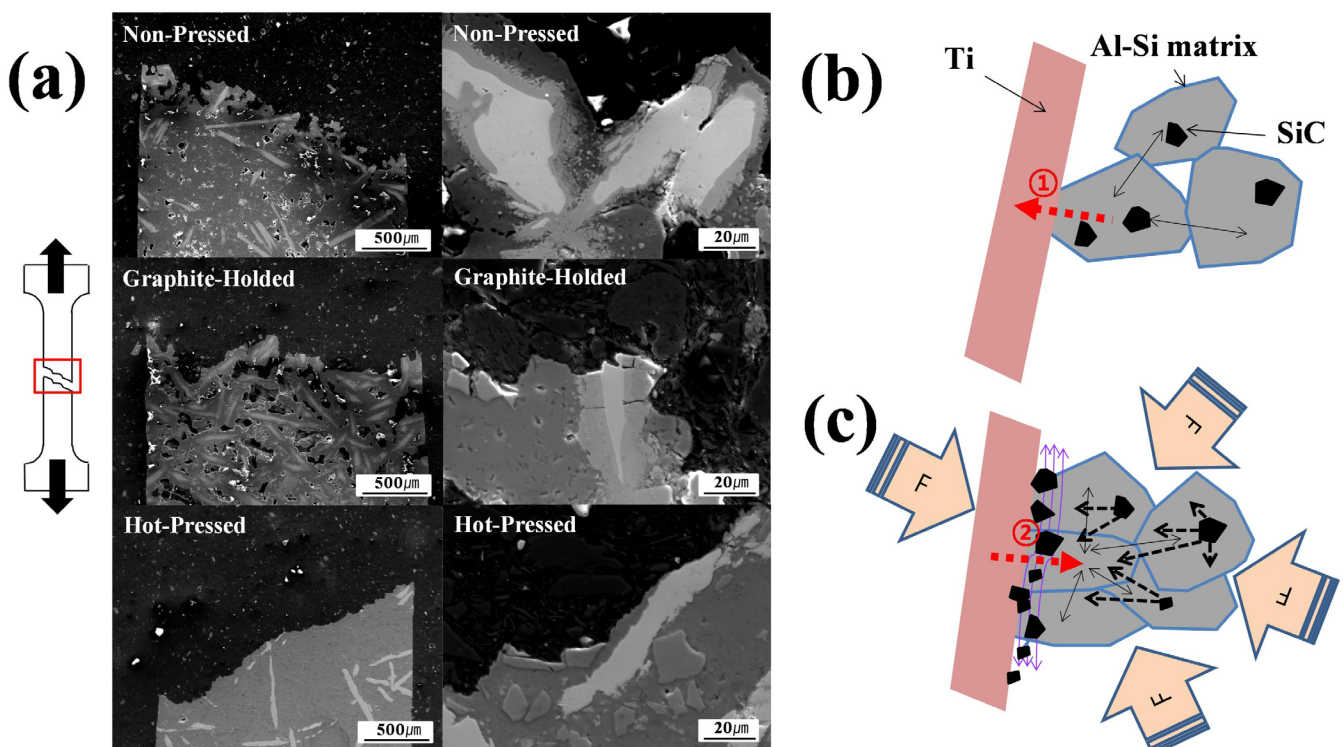

Fig. 8. Lateral morphologies of tensile tested specimens with the highest strength in each sintering method (a), schematic illustrations of the sintering condition by Fig. 2a type method (b) and Fig. 2b type method (c)
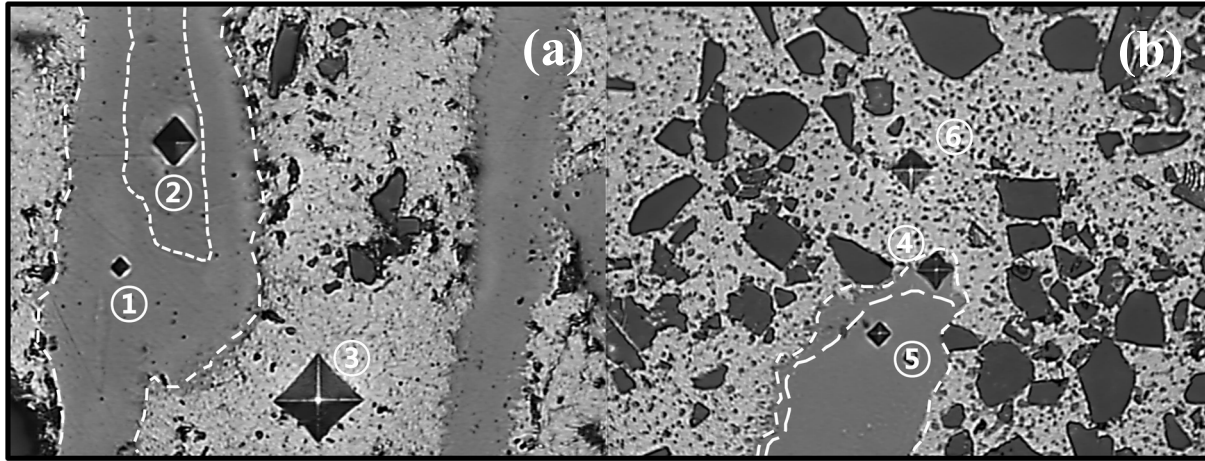
Fig. 9. FE-SEM images of Vickers hardness test traces in each phase of the sintered specimens: (a) graphite-holded 95A5T specimen and (b) hot-pressed 85A15T specimen

TABLE 2

Vicker's hardness values of the related phases
in the sintered specimens in Fig. 9

Position	1 ($Ti_7Al_5Si_{12}$)	2 (Ti)	3 (Al-Si)	4 (Ti-Al)	5 (Ti)	6 (Al-Si)
Hardness (Hv)	858.4	183.9	52.8	80.1	187.4	62.7

In case of formation of this ternary phase, there are directional property of solid solubility and atomic substitution. Al-Si phase →$Ti_7Al_5Si_{12}$ phase → Al-Si phase and Ti-Al phase → solid Ti diffusional reaction at interface boundary is the direction of easy flow because Al-Si(FCC), $Ti_7Al_5Si_{12}$ (BCT) and Ti (HCP) have a_{Al}: 4.049Å, a_{Si}: 5.392Å, $a_{Ti7Al5Si12}$:3.57Å and a_{ti}:2.95Å in the view of structure, respectively. Direction of Al or Al-Si→$Ti_7Al_5Si_{12}$ has match between Al or Al-Si and $Ti_7Al_5Si_{12}$ in crystallization. On the contrary to this, direction of Ti → $Ti_7Al_5Si_{12}$ has mismatch between Ti and $Ti_7Al_5Si_{12}$ in crystallization.

At condition of isothermal static pressure compression such as the non-pressed and graphite-holed conditions in this study, diffusion system is to be Ti-rich corner as shown in Fig. 8b, solid solution worked form Al-Si matrix into Ti matrix, negative mixing enthalpy and atomic radii effect of Si for Ti is significant (Si-rich phase). Diffusion zone is formed mainly $Ti_7Al_5Si_{12}$ phase. In case of the inhibited formation of this ternary phase, the increased local thermal stress by hot-press process makes to accelerate flow-viscosity and increase mobility of Al-Si matrix and SiCp lead to heterogeneous phase growth in interfacial zone. There needs Si source of supply and time for generation of $Ti_7Al_5Si_{12}$ phase. But generated flow-viscosity diffusion environment between Ti-fiber and main matrix increased frequency of Al contact with Ti and the accelerated dispersibility of Al-Si phase and SiCp lead to heterogeneous phase growth.

At condition of isothermal dynamic pressure compression such as the hot-pressed conditions, diffusion system is to be Al-rich corner as shown in Fig. 8c, high flow-viscosity solid solution worked form Ti matrix into Al-Si matrix, Al-9Si eutectic like phase provided high-volume Al and a small quantity of Si to Ti [29]. Therefore, diffusion zone is formed mainly TiAl phase as follows; solid Ti(HCP a_{ti}:2.95Å, c_{Ti}: 4.682 Å) phase → TiAl(FCT a_{TiAl}:2.837Å, c_{Ti}: 4.059 Å) phase → Al-Si(FCC a_{Al}: 4.049Å, a_{Si}: 5.392Å) phase diffusional reaction at interface boundary in this study.

To comprehensively evaluate the relative mechanical properties in each sintered specimen, there was highly relevant with interfacial reaction products. In addition, it reveals that diffusion direction may be varied by sintering method such as from Ti-rich corner to Al-rich corner matrix in this study.

4. Conclusion

We have successfully produced the two-step reinforced Al-based MMCs in this study. These composites demostrate high mechanical strength and wide plastic deformation, which may allows its subsequent reinforcing structure on sintering porocess with multi-diffuion layer. The improved Al-based MMC studied has a potentiality to be applied for sprocket materials in automobile by various sintering methods. The obtained comprehensive results are summarized as follows:

1. Gas atomized Al-Si/SiCp powder has an advantage for decentrally-organized SiCp were existed inside of Al-Si powders as proposed and the clustering of SiCp was prevented.

2. The reacted layer between Ti-fiber and Al-Si matrix was formed by each sintering method and these diffusion layers have effect to change of mechanical properites by amount of Ti-fiber and sintering methods.

3. Intermetallic compound $Ti_7Al_5Si_{12}$ ternary phase was formed at interfacial zone contacted with Ti-rich corner matrix and this phase was not observed at at interfacial zone contacted with Al-rich corner matrix. Direction of progress of phase formation is Al–9Si phase → $Ti_7Al_5Si_{12}$ → AlSi phase and TiAl phase → solid Ti phase in Ti-rich corner matrix and solid Ti phase → TiAl phase → Al-Si phase in Al-rich corner matrix, respectively.

4. Tensile strength and elongation in the hot-pressed specimens by 2step-reinforcement were improved in 19.5% and 26.2% more than those of Al-Si/SiCp. TiAl phase was much more effective than $Ti_7Al_5Si_{12}$ phase for strength and plastic deformation enhancement.

5. It reveals that diffusion direction changed by sintering methods at low temperature in this study.

REFERENCES

[1] W.S. Miller, L. Zhuang, J. Bottema, A. Wittebrood, P. De Smet, A. Haszler, A. Vieregge, Mat. Sci. Eng. A **280**, 37 (2000).

[2] P. Kapranos, D.H. Kirkwood, H.V. Atkinson, J.T. Rheinlander, J.J. Bentzen, P.T. Toft, C.P. Debel, G. Laslaz, L. Maenner, S. Blais, J.M. Rodriguez-Ibabe, L. Lasa, P. Giordano, G. Chiarmetta, A. Giese, J. Mater. Process. Tech. **135**, 271 (2003).

[3] Z.X. Liang, B. Ye, L. Zhang, Q.G. Wang, W.Y. Yang, Q.D. Wang, Mater. Lett. **97**, 104 (2013).

[4] M. Gupta, S. Ling, J. Alloy. Compd. **287**, 284 (1999).

[5] G. Chirita, D. Soares, F S. Silva, Mater. Des. **29**, 20 (2008).

[6] O.E. Sebaie, A.M. Samuel, F.H. Samuel, H.W. Doty, Mat. Sci. Eng. A **480**, 342 (2008).

[7] S. Scudino, G. Liu, M. Sakaliyska, K.B. Surreddi, J. Eckert, Acta Mater. **57**, 4529 (2009).

[8] S.Q. Wu, Z.S. Wei, S.C. Tjong, Compos. Sci. Technol. **60**, 2873 (2000).

[9] G.H. Zhang, J.X. Zhang, B.C. Li, W. Cai, Prog. Nat. Sci. **21**, 380 (2011).

[10] S. Tzamtzis, N.S. Barekar, N. Hari Babu, J. Patel, B.K. Dhindaw, Z. Fan, Compos. Part A-Appl. S. **40**, 144 (2009).

[11] G. Miranda, M. Buciumeanu, S. Madeira, O. Carvalho, D. Soares, F.S. Silva, Compos. Part B-Eng. **74**, 153 (2015).

[12] X.Y. Huang, C.M. Liu, X.J. Lv, G.H. Liu, F.Q. Li, J. Mater. Process. Tech. **211**, 1540 (2011).

[13] A. Arias, R. Zaera, J. López-Puente, C. Navarro, Compos. Struct. **61**, 151 (2003).

[14] S. Naher, D. Brabazon, L. Looney, Compos. Part A-Appl. S. **38**, 719 (2007).

[15] A. Fujiki, Mater. Chem. Phys. **67**, 298 (2001).

[16] D.P. Bishop, J.R. Cahoon, M.C. Chaturvedi, G.J. Kipouros, W.F. Caley, Mater. Sci. Eng. A **290**, 16 (2000).

[17] N. Showaiter, M. Youseffi, Mater. Des. **29**, 752 (2008).

[18] S.S. Su, I.T.H. Chang, W.C.H. Kuo, Mater. Chem. Phys. **139**, 775 (2013).

[19] H.K. Lee, Korean J. Mater. Res. **23**, 574 (2013).

[20] Y. Li, Q. Luo, J.Y. Zhang, Q. Li, in "Light Metals 2013", p. 391. John Wiley & Sons, Inc., 2013.

[21] O. Dezellus, B. Gardiola, J. Andrieux, M. Lomello-Tafin, J.C. Viala, J. Phase. Equilib. Diff. **35**, 137 (2014).

[22] X.G. Chen, M. Fortier, J. Mater. Process. Tech. **210**, 1780 (2010).

[23] N. Saheb, T. Laoui, A.R. Daud, M. Harun, S. Radiman, R. Yahaya, Wear **249**, 656 (2001).

[24] M. Zeren, E. Karakulak, J. Alloy. Compd. **450**, 255 (2008).

[25] A.C. Ferro, B. Derby, Acta Metall. Mater. **43**, 3061 (1995).

[26] D. Walter, I.W. Karyasa, J. Chin. Chem. Soc-Taip **52**, 873 (2005).

[27] S. Anand, T.S. Srivatsan, Y. Wu, E.J. Lavernia, J. Mater. Sci. **32**, 2835 (1997).

[28] A. Inoue, Y. Kawamura, H.M. Kimura, H. Mano, Metastable, Mechanically Alloyed and Nanocrystalline Materials, Ismanam-2000, Mater. Sci. Forum **360-3**, 129 (2001).

[29] Q. Luo, Q. Li, J.Y. Zhang, S.L. Chen, K.C. Chou, J. Alloy. Compd. **602**, 58 (2014).